Applied Catalysis B: Environmental 236 (2018) 99–106

Contents lists available at ScienceDirect

Applied Catalysis B: Environmental

journal homepage: www.elsevier.com/locate/apcatb

Carbon nitride with electron storage property: Enhanced exciton dissociation for high-efficient photocatalysis

Zhenxing Zeng, Xie Quan*, Hongtao Yu, Shuo Chen, Yaobin Zhang, Huimin Zhao, Shushen Zhang

Key Laboratory of Industrial Ecology and Environmental Engineering (Ministry of Education), School of Environmental Science and Technology, Dalian University of Technology, Dalian 116024, China

ARTICLE INFO

Keywords:
Carbon nitride
Electron storage
Excitonic effect
Exciton dissociation
Artificial photosynthesis

ABSTRACT

Excitonic effect, originated from the strong Coulomb attraction between electron and hole, plays an important role in the photocatalytic process of polymeric materials but has been long ignored. In view point of hot-carriers generation, the dissociation of Frenkel excitons is proposed as an effective way to improve the photocatalytic performance of polymeric photocatalysts. Herein, by taking graphitic carbon nitride (g-C_3N_4) as an example, we verify that endowing g-C_3N_4 with electron storage ability can facilitate exciton dissociation by extracting electrons from bound electron-hole couples around the electron stotage sites, therefore enhancing the hot-carriers harvest and suppressing the charge recombination. Benefiting from these advantages, the as-prepared material demonstrates excellent photocatalytic performance for both H_2 evolution and H_2O_2 generation. As a result, the apparent quantum yield (AQY) for H_2 evolution at 420 nm reaches 55%, which is much higher than most of the reported polymeric materials. The study described here offers a new way for designing advanced polymeric photocatalysts toward high performance solar energy conversion via excitonic engineering.

1. Introduction

Artificial photosynthesis, an important catalytic reaction to convert the abundant solar energy into renewable fuels, has long been considered as a promising way to address the energy crisis and to deal with the environmental issues [1–3]. Graphitic carbon nitride (g-C_3N_4) as a metal-free photocatalyst has shown its promise for photocatalysis by virtue of its unique properties, such as visible-light response, physicochemical stable, suitable energy structure for water splitting and easy regulation [4–6]. For this reason, various g-C_3N_4 based photocatalytic devices in the past few decades have been built for solar energy conversion [7–10]. For polymeric photocatalyst, it is believed that the photocatalytic activity is closely related to the generation of hot electrons and holes [11–13]. However, unlike the inorganic semiconductors with strong screening effects and large dielectric properties, most of the polymeric materials including g-C_3N_4 exhibit strong Coulomb interaction between the electron and hole [14,15]. In this context, the photogenerated electrons and holes in the polymeric materials are in the form of neutral bound couples (known as Frenkel exciton) with large binding energy, which greatly hinders the dissociation of Frenkel excitons into hot electrons and holes for the subsequent catalytic reactions [16]. As a result, g-C_3N_4 displays a high charge recombination rate and therefore presents rather low photocatalytic activity. To improve the photocatalytic performance of g-C_3N_4, it is necessary to explore alternative ways to facilitate the dissociation of excitons for hot-carriers generation.

In natural photosynthesis of green plants, the photogenerated excitons are efficiently dissociated by in situ electron storage in the form of ATP or NADPH, while holes are consumed by water oxidation to produce molecular oxygen [17–20]. Subsequently, the stored electrons are then transferred to the reaction sites and used as driven energy for hydrocarbons synthesis [21,22]. Such an electron storage and transfer process not only can guarantee the dissociation of excitons to generate adequate hot-carriers, but also can minimize the recombination of electron-hole, that's why the photosynthetic performance of plants is that high. In this procedure, the electron storage process by decoupling the redox reactions is the core part for excitons dissociation. So, it is reasonable to deduce that endowing g-C_3N_4 with electron storage ability should be a possible way to simulate such process for exciton dissociation. In our concept, owning to the electron storage character, the electron storage sites may provide a driving force (similar to the magnetic force) to extract electrons from excitons and thus facilitating the dissociation of excitons. Moreover, holes can be consumed by hole scavenger, therefore temporarily decoupling the redox reactions to minimize electron-hole recombination (as illustrated in Scheme 1). Furthermore, the trapped electrons can be also transferred to the

* Corresponding author.
E-mail address: quanxie@dlut.edu.cn (X. Quan).

https://doi.org/10.1016/j.apcatb.2018.05.003
Received 1 March 2018; Received in revised form 25 April 2018; Accepted 2 May 2018
Available online 03 May 2018

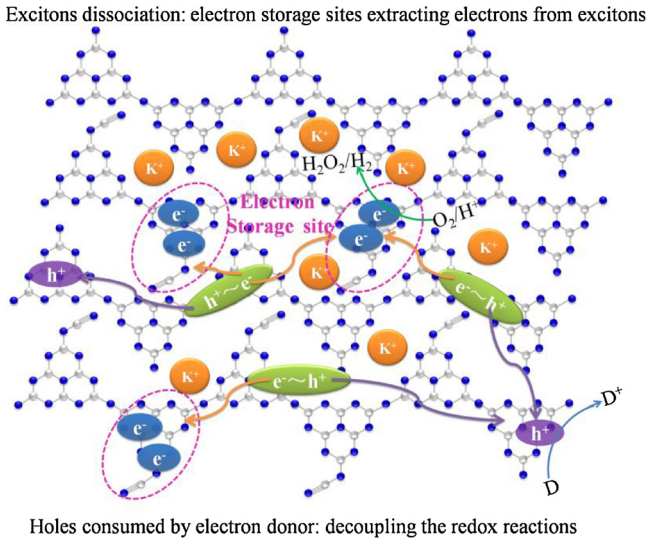

Scheme 1. Schematic illustration of electron storage facilitated exciton dissociation and charge transfer in CCN.

reactive sites for fuels synthesis, therefore forming a dynamic equilibrium between the excitons dissociation and the consumption of trapped electrons [21,23]. In this regard, the sluggish excitons dissociation for hot-carriers generation and severe electron-hole recombination drawbacks can be largely improved, simultaneously.

In the present study, we successfully rendered g-C_3N_4 with electron storage ability by installing it with cyano-groups through an ionothermal treatment. Taking this cyano-groups modified g-C_3N_4 (CCN) as an example, we propose a novel electron storage strategy for excitons dissociation and for the suppression of electron-hole recombination. Endowing it with electron storage ability not only can facilitate exciton dissociation for hot electrons and holes generate, but also can decouple the redox reactions for minimizing electron-hole recombination. Remarkably, owning to the enhanced Frenkel excitons dissociation efficiency together with the reduced electron-hole recombination, the as-prepared CCN exhibits excellent photocatalytic performances for H_2 evolution and H_2O_2 generation. After further optimizing the electron storage ability, a nearly two-magnitude enhancement is observed on CCN (508 μmol/h) than that of g-C_3N_4 (5.1 μmol/h) with apparent quantum yield (AQY) reaches 55% for H_2 evolution at 420 nm, higher than most reported polymeric materials.

2. Experimental section

2.1. Synthesis of g-C_3N_4

In typically, 10 g of melamine was put into a crucible with a cover and heated to 550 °C in a muffle at a heating rate of 12 °C/min and hold at this temperature for another 4 h, the yellow powder was obtained after natural cooling to room temperature.

2.2. Synthesis of CCN

10 g of melamine was put into a crucible with a cover and heated to 500 °C in a muffle at a heating rate of 12 °C/min and then holding this temperature for 4 h to form melon. Then 500 mg of pretreated melamine and 6 g of a eutectic composed of KCl and LiCl (with a fixed weight ratio of 11:9) were mixed, subsequently, the fine grounded mixture were put into a crucible with a cover and heated to 550 °C and maintained this temperature for 4 h under Ar atmosphere at a heating rate of 12 °C/min. The final material was obtained by drying the water washed powder at 60 °C overnight.

2.3. Synthesis of CCN with different introduced amount of cynao groups

CCN with different introduced amount of cynao groups were synthesized using the same condition as CCN, except for the adding amount of eutectic salts. The obtained sample was labeled as CCN-x, where x = (1, 2, 3, 4) refer to the mass of eutectic as 0.22, 0.67, 3.0, and 12 g, respectively.

2.4. Photoreaction

Photocatalytic H_2O_2 production reactions were carried out under visible light by dispersing 50 mg of as prepared material into 100 mL of an aqueous solution containing 10 mL of methanol. Photocatalytic water splitting reactions were carried out in a Pyrex top-irradiation reaction vessel connected to a glass closed gas system. Before the hydrogen evolution reactions, 3 wt% of Pt was loaded on to the surface of as prepared materials. In a typical process, 50 mg of Pt loaded catalyst was dispersed into 100 mL of an aqueous solution containing 10 mL of methanol. Prior to the irradiation, the system was evacuated for several times to completely remove the residual air. The evolved gases were analyzed by a TCD and 5 Å molecular sieve column equipped gas chromatograph (GC-14), argon was used as carrier gas. Visible light was served by a 300 W Xenon lamp by employing a long pass wavelength filter of $\lambda > 420$ nm. The temperature of the reaction system was maintained at 10 °C using a flow of cooling water.

2.5. Dark reaction

50 mg of as-prepared material was dispersed into 50 mL of an aqueous solution containing 10 mL of methanol and then the system was evacuated for several times to completely remove the residual oxygen. The evacuated system was irradiated under simulate sunlight irradiation for 2 h to form a blue colored suspension and then the reactor was kept in dark. Specific electron acceptor was injected into the system for selective production of H_2 or H_2O_2 (Pt for H_2 evolution, O_2 for H_2O_2 evolution).

3. Results and discussion

CCN with electron storage ability was fabricated using a modified ionothermal synthesis strategy [24,25]. First, melamine was pre-polymerized in a muffle to form melon. Subsequently, the as-obtained melon was ground with a eutectic mixture of LiCl and KCl to form uniform mixture, followed by treating the mixture under argon condition at 550 °C to install it with cyano-groups so as to endow the material with electron storage ability. The presents of LiCl and KCl is probably used etch g-C_3N_4 to opening the CN heterocycle so as to installing the material with cyano-groups and to render the framework negative charged and compensated by K^+. The eutectic salts with low melting point make it possible for uniformly modifying the material and it's vital to render g-C_3N_4 with electron storage ability [24,25]. As a reference, g-C_3N_4 was prepared by the direct polymerization of melamine. Details for the materials synthesis is given in the Experimental Section. The structural information of as-prepared CCN and g-C_3N_4 were firstly investigated by X-ray diffraction (XRD). XRD patterns in Fig. 1a show that both samples display two distinguish peaks but show different locations. Different with g-C_3N_4, the interlayer stacking corresponded peak of CCN moves to higher diffraction angle while the in-plane repeating motif indexed peak shift to lower diffraction angle, respectively attribute to the enhanced regularity of interlayer stacking and more stretched in-plane structure [4, 24]. In addition, the decreased diffraction peaks intensity of CCN may attribute to the thermal exfoliation effect of the molten salts treatment (Fig. S1).

The chemical structure of CCN was further investigated by FT-IR and XPS measurements. Apart from the typical carbon nitride skeleton (801 cm^{-1} for triazine vibration and 1000–1700 cm^{-1} for the vibration

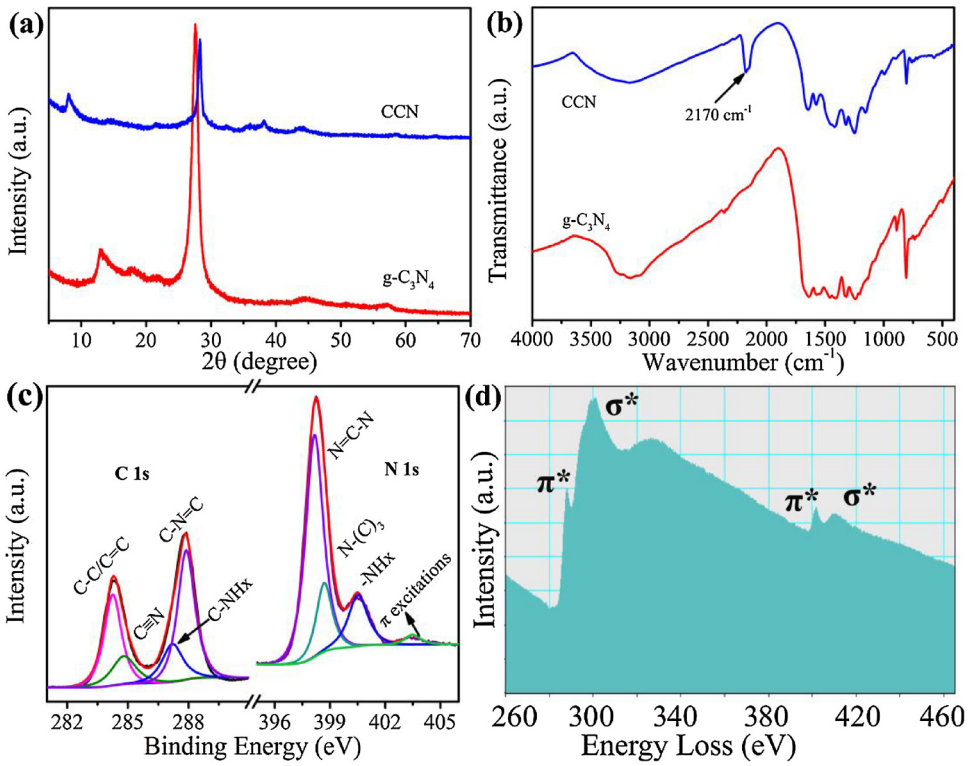

Fig. 1. (a) XRD patterns and (b) FT-IR spectra of g-C_3N_4 and CCN. (c) C 1s and N 1s XPS spectra and (d) EELS spectra of CCN.

of aromatic CN heterocycles), CCN shows two new vibration peaks located at 2170 and 1056 cm^{-1} (Fig. 1b). The former one is assigned to the vibration of cyano-groups whereas the later one may refer to the NC_2 bonds asymmetric vibration of metal-CN_2, demonstrating the successful modification of CCN with cyano-groups and the presence of K−CN_2 bond [25,26]. Furthermore, a N/C ratio loss is observed on CCN, suggesting the introduction of nitrogen vacancy during the post-synthetic process (Table S1) [9]. In Fig. 1c, the C 1s spectrum of CCN can be fitted into four deconvoluted peaks located at 284.3, 284.8, 287.2 and 287.2 eV, respectively corresponding to graphitic carbon (C−C/C═C), C≡N bond, primary or secondary amines (C−NHx) and sp^2 hybridized C atoms (C−N═C). For the N 1s spectrum, the spectrum can also be fitted into four peaks at 398.1, 398.7, 400.5 and 403.5 eV, respectively. The presence of C≡N bond in the C 1s and N 1s spectra also confirms the presence of introduced cyano-groups. The low intensity peak located at 403.5 eV is assigned to the charging effect of the heterocycles; the peak located at 398.1 eV is for sp^2 hybridized aromatic N bonded to carbon atoms (C═N−C), whereas the peak at 399.7 eV is assigned to the tertiary N bonded to carbon atoms in the form of N−$(C)_3$ and the peak located at 400.7 eV is for amino functions caring hydrogen (C−NHx). The similar C 1s and N1s spectra between CCN and g-C_3N_4 demonstrate the typical carbon nitride skeleton has not changed after the ionothermal treatment (Fig. S2). In addition, the high resolution K 2p spectrum presents two peaks with binding energy located at 393.0 eV and 295.7 eV, again confirming the incorporation of K [27,28]. It can be seen from the K 2p XPS spectra in Fig. S3, the high resolution K 2p spectra before and after different Ar^+ plasma etching times are quite similar, suggesting the homogeneous doping of K^+. As we know that carbon nitride is a polymeric material with typical layered structure, the detected K^+ on the surface and bulk suggesting that the introduced K^+ should be located between the layers [29–31]. The interaction between layers and the K^+ may constitute a possible explanation to the shifted XRD peak of (002) plane (see in Fig. 1a). Furthermore, Zeta potential of CCN (Fig. S4) is more negative than that of pristine g-C_3N_4 [27], indicating the negative nature of the framework, suggesting that the K^+ within CCN may just function as charge compensation.

Electron energy loss (EELS) characterization was employed to further uncover the structural information of as-prepared CCN. The EELS spectrum of CCN in Fig. 1d displays a sharp carbon K-ionization and nitrogen K-ionization edge peaks located at 285.6 eV and 401 eV, respectively. The peaks located at 285.6 eV and around 300 eV respectively refer to the electron transition from the core 1s to π* and electron from the orbital 1s to σ*, which demonstrates the presence of sp^2 hybridized carbon atom that bonded to nitrogen [32,33]. Similarly, the peak located at 401 eV is attributed to the sp^2 hybridized nitrogen. In this regard, it is clear that the CCN is composed of sp^2 hybridized carbon and nitrogen, revealing the typical sp^2 hybridized heptazine structure remained after molten salt treatment. The structure difference between CCN and g-C_3N_4 may just lies in the introduction of cyano-groups and compensation of negative charged framework with K^+ ions.

As for photocatalysis, CCN changes color from pristine yellow to blue when the degassed system was subjected to light irradiation, in the presence of electron sacrificial reagents such as methanol, TEOA, IPA and 4-methylbenzyl alcohol (4-MBA) (Figs. 2a and S5). Interestingly, the blue color can be restored to the initial yellow when air backfilled into the system, indicating the color change is switchable. In sharp contrast, no obvious change can be observed on g-C_3N_4. Details for the color change was further investigated by UV/Vis diffuse reflectance spectra (DRS). As shown in Fig. 2b, prior to light irradiation, both g-C_3N_4 and CCN display only one adsorption band with onset around 470 nm. After light irradiation, CCN turns blue and exhibits a broad absorption in the range of 490–750 nm, in good agreement with the presented blue color of CCN. It was reported that the switchable color change between yellow and blue is originated from the electron accumulation on carbon nitride and usually act as an indicator for electron accumulation [21,23]. In the current system, the switchable color change should also refer to the successful attachment of CCN with electron storage ability. To confirm the switchable color change between blue and yellow is originated from the electron accumulation on the material, open circuit photovoltage (OCP) measurement (Fig. 2c) was performed. The OCP experiment was carried out in a

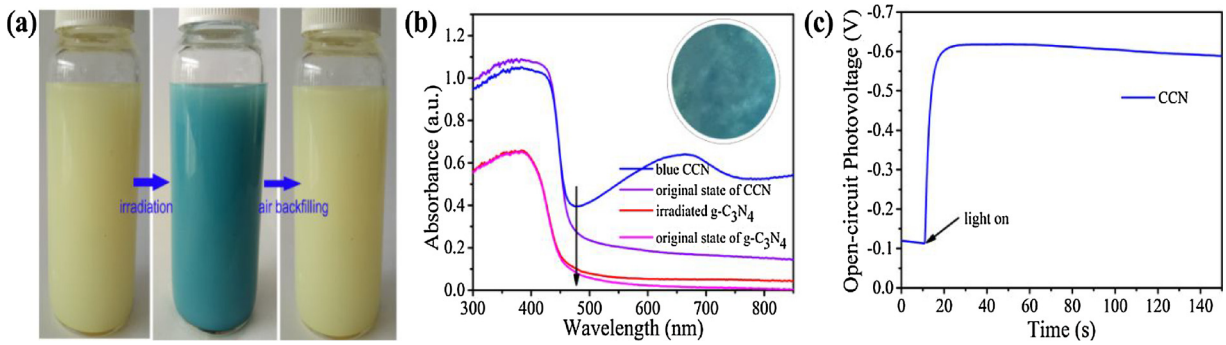

Fig. 2. (a) Photographs of CCN suspension before irradiation, after irradiation and after air backfilling. (b) UV/vis Diffuse reflectance spectra of g-C_3N_4 and CCN. (c) Open circuit photovoltage of CCN.

photoelectronchemical cell by using 0.1 mol/L Na_2SO_4 containing appropriate amount of TEOA as electrolyte. Before testing, the system was bubbled with N_2 to remove the dissolved O_2. When light switched on, the color of CCN on FTO changed from yellow to blue with the OCP reaches near −600 mV, further confirming that the blue color switch is originated from the electrons accumulation. However, a slightly decrease of the OCP is observed which may attribute to the residual O_2 in the solution [21]. These results not only demonstrate the successful attachment of CCN with electron storage ability, but also tell the truth that the stored electrons on CCN were highly reductive.

The electron storage feature of CCN is supposed to be closely related to the Frenkel exciton dissociation process. So, steady-state photoluminescence (PL) and time-resolved photoluminescence measurements (TR-PL) were then performed to investigate the associated exciton dissociation process. As shown in Fig. 3a, CCN exhibits significantly reduced emission wavelength (470 nm) intensity than that of g-C_3N_4. As PL originates from the recombination of the singlet exitons, the sharply reduced emission intensity means the remarkably decreased population of exitons, which is ascribed to the enhanced excitons dissociation and therefore presents suppressed charge recombination [11,34,35]. To better understanding the involved exciton dissociation process, TR-PL measurements was performed to show the prompt radiative decay of the excitons. As displayed in Fig. 3b, the emission decay curves of g-C_3N_4 and CCN were fitted using the biexponential kinetics function, where two decay components of τ_1 and τ_2 are derived (details for the lifetimes components are shown in Table S2). The shorter lifetime component of τ_1 is originated from the nonradiative quenching, whereas the longer one of τ_2 represents the recombination of free excitons in the materials. For CCN, the emission lifetimes of both components (τ_1 = 0.49 ns, τ_2 = 3.554 ns) are shorter than that of g-C_3N_4 (τ_1 = 1.35 ns, τ_2 = 6.37 ns). The significantly quenched emission intensity and shortened PL lifetimes respectively represents the reduced exciton population and the electron-hole recombination, indicating the enhanced exciton dissociation on CCN [11,16,25,35]. As a representative of the overall decay behavior, the average PL lifetime of CCN (1.2 ns) also display a decrease than that of g-C_3N_4 (3.9 ns). The observation of PL quenching together with the PL lifetimes reduction confirms the enhanced exciton dissociation on CCN.

In view of the enhanced exciton dissociation, the electron behavior on CCN is therefore different from that of g-C_3N_4. The stored electrons on the materials were further investigated by the dark catalytic H_2 evolution and H_2O_2 generation, respectively. After charging the CCN

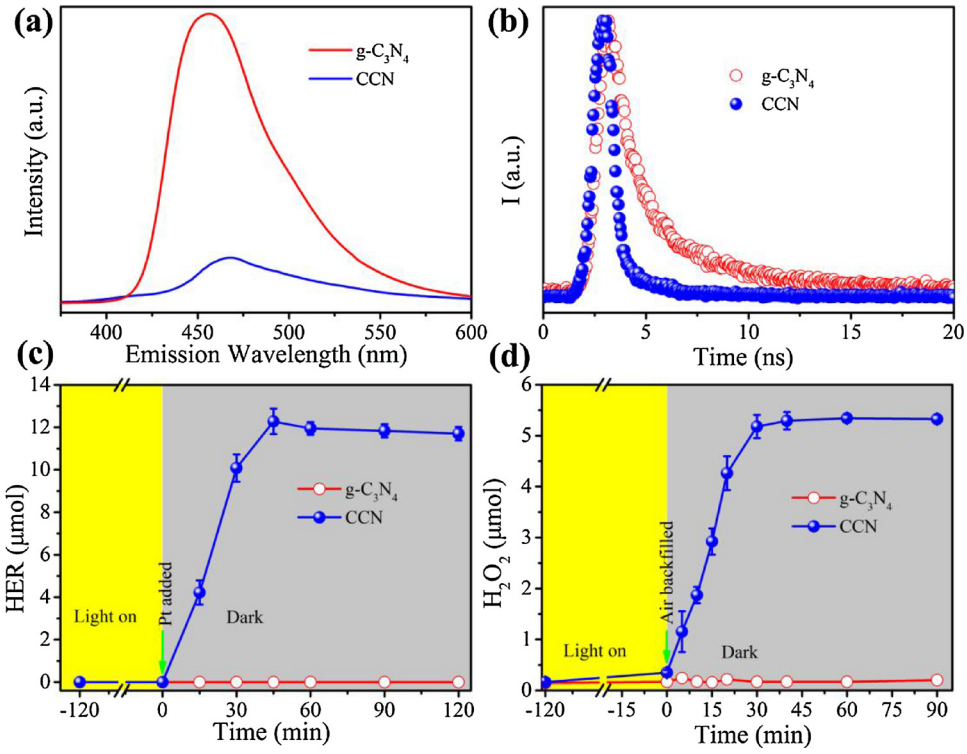

Fig. 3. (a) Steady-state PL spectra and (b) Time resolved PL spectra of g-C_3N_4 and CCN. Dark catalytic performance of photo charged g-C_3N_4 and CCN for (c) H_2 and (d) H_2O_2 production. Note: as for the dark H_2 production, 3 wt% of Pt nanoparticles solution was injected into the photo charged system, while air backfilling for H_2O_2 generation.

with light irradiation, the suspension turned blue and maintained this state without any other changes for days under anaerobic condition (Fig. S6), indicating the high stability of the trapped electrons. After irradiation, the system was subjected to dark by wrapping the reactor with tinfoil. For H_2 evolution, a certain amount of Pt nanoparticles solution was injected into the system. As shown in Fig. 3c, after reaction for near an hour the produced H_2 reached maximum amount of near 12 μmol, while the blue color of the suspension backed to the pristine yellow, revealing that the stored electrons were exhausted. As a control, neither color change nor H_2 was observed or tested for g-C_3N_4, indicating none electron storage nature of it. When air instead of Pt nanoparticles was injected into the system, a similar color change was observed. Besides, more than 5 μmol H_2O_2 was detected in the suspension (Fig. 3d). On the basis of the produced amount of H_2, the electron concentration of CCN and g-C_3N_4 was respectively estimated to be 24 μmol and 0 μmol (assuming that all the trapped electrons are used for H_2 evolution). Based on the above results, we verify that CCN with electron storage could favor excitons dissociation and suppressing electron-hole recombination, thereby showing the electron accumulation in the material.

On the basis of the above analysis, the exciton dissociation process for catalytic reaction is shown in Scheme 1. Upon light irradiation, photogenerated excitons are trend to be dissociated around the electron storage sites by extracting electrons from excitons, while holes can be consumed by hole scavenger. In this regard, the exciton dissociation process can be reflected by the electron accumulation process and visualized by the gradually color change from pristine yellow to blue. Once one hole is quenched by methanol, one electron is stored within the material. The continuous consumption of holes will result in the electron accumulation within the material. The electron accumulation will lead to the color change of the material, the deeper the color, the higher the electron concentration. Once the material reaches its maximum electron storage capacity, the color will not change any more and present as deep blue. As shown in Fig. S7, the gradually color change from pristine yellow to the blue and finally maintained blue without any other change strongly support this claim.

Owning to the enhanced exciton dissociation and suppressed electron-hole recombination, CCN is expected to display high photocatalytic performance. The photocatalytic activity of CCN and g-C_3N_4 were then examined by visible light half water splitting to produce H_2 and O_2 reduction to generate H_2O_2. Prior to the H_2 production experiments, 3 wt% of Pt was loaded onto the surface of CCN to boost H_2 evolution. Owning to the enhanced exciton dissociation and inhibited electron-hole recombination, CCN exhibits an excellent visible-light-driven H_2 evolution performance at a rate of 45 μmol/h (Fig. 4a), which is almost 15 times higher than that of pristine g-C_3N_4. The H_2O_2 generation experiments were also carried out in an open wide reactor without modifying any noble metal nanoparticles (Fig. 4b). Remarkably, CCN shows an exceptional visible-light-driven photocatalytic performance for H_2O_2 production at a rate of 210 μmol/h, which is more than 35-fold higher than that of g-C_3N_4 (6.0 μmol/h). To clarify that this outstanding performance is mainly contributed from the electron storage process rather than the contribution from the structure change, the reference material with structurally similar to CCN but without electron storage ability was prepared (donated as CCN-R). As shown in Fig. S8, compared with g-C_3N_4 although the structure change can improve the photocatalytic performance (4 times), but it is still far more less than the enhancement contributed by the electron storage process (12.6 times), highlighting the significant contribution of the electron storage property. We also noticed the phenomenon that CCN maintains light blue color during the photocatalytic H_2 evolution. As the blue color change originated from the electron accumulation on the material, this result also indicates that the photogenerated excitons should be firstly dissociated with electrons stored in the electron storage sites and then the trapped electrons transferred to platinum nanoparticles for H_2 production.

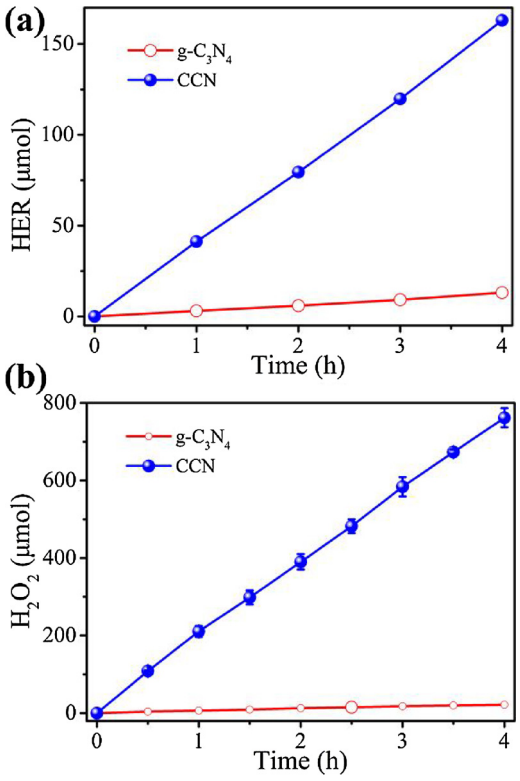

Fig. 4. (a) Photocatalytic H_2 evolution and (b) H_2O_2 production over g-C_3N_4 and CCN, respectively. Note: methanol was used as sacrificial reagent for H_2 and H_2O_2 synthesis.

As the exciton dissociation is closely related to the electron storage property, it is necessary to interpretate the electron storage mechanism for the guidance of further improving the catalytic performance of CCN. The structural difference between CCN and g-C_3N_4 from the structural characterization results suggests that the electron storage ability of CCN is endowed by modifying the K^+ ion compensated framework with cyano-groups. To verify this claim, controlled experiments were then performed to show the importance of these two factors. Firstly, the cyano-groups were wiped off by hydrolyzing it in acid solution; secondly, $NaBH_4$ was used as H_2 source so as to install g-C_3N_4 with cyano-groups (Fig. S9) [36–38]. Interestingly, both samples don't show any color change, revealing none electron trapping ability of these two materials. Besides, adding K^+ into the solution cannot endow the cyano-groups modified g-C_3N_4 with electron storage ability. It seems that both cyano-groups and K^+ compensation of the negative charged framework are essential to form the special structure for gaining electron storage feature. Furthermore, it was reported that tri-s-triazine ring modified with partly neutral and partly negative charged tri-s-triazine rings can hold a stable structure for electrons location [4,21]. So, it is plausible that the electron storage ability is endowed by modifying the tri-s-triazine ring with one neutral cyano-groups, where this tri-s-triazine ring is neighbored two negative charged cyano-group modified tri-s-triazine rings (the possible structure of CCN is shown in Fig. S10). In addition, the homogeneous intercalation of K^+ within the carbon nitride layers (Fig. S11) may result in the stable existence of trapped electrons, just like the H^+ intercalation to stabilizing the trapped electrons on TiO_2 [39,40]. That's why the stored electrons on CCN can stably persist for such a long time (Fig. S6). To this end, it is clear that the introduced cyano-groups and K^+ ions are two core factors that affect the electron storage property.

Since the electron storage character can greatly affect the exciton dissociation process, expanding the electron storage capacity may accelerate the exciton dissociation process due to the increased electron

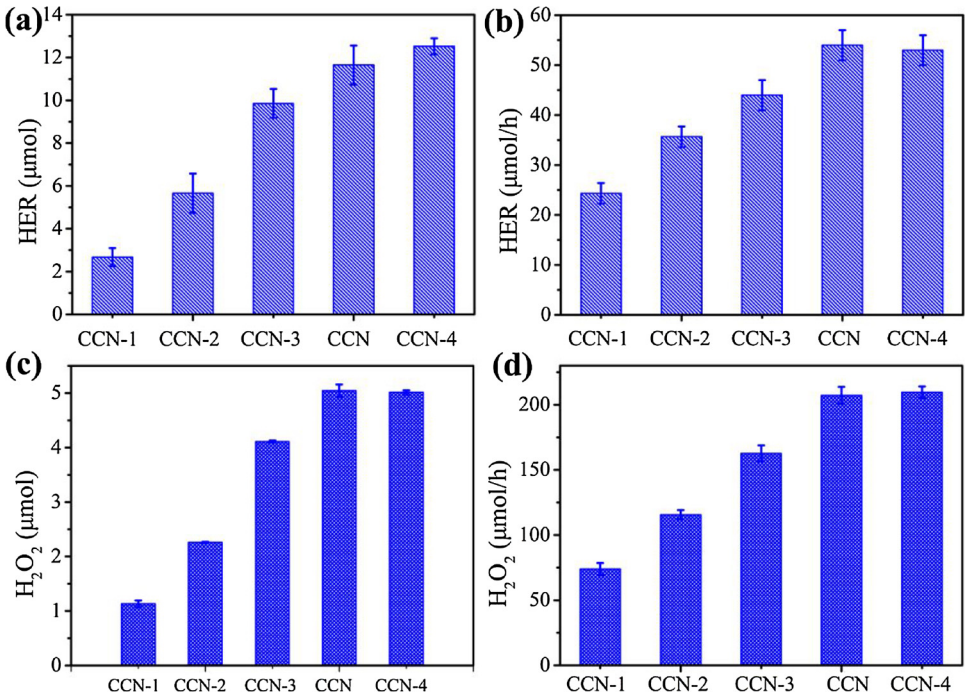

Fig. 5. (a) Dark H_2 evolution and (b) photocatalytic H_2 evolution over CCN_X. (c) Dark H_2O_2 generation and (d) photocatalytic H_2O_2 generation over CCN_X. Note: as for the dark H_2 production, 3 wt% of Pt nanoparticles solution was injected into the system. Unless otherwise stated, methanol was used as sacrificial reagent.

acceptance of electron storage sites. Here, a series of CCN materials with different amount of introduced cyano-groups were fabricated and the electron storage capacity was evaluated by converting the electrons into H_2 or H_2O_2. Fig. S12 shows the successful control of the introduced amount of cyano-roups. As we can see in Fig. 5a, the electron storage capacity increases with the increasing amount of introduced cyano-groups, demonstrating the successful control of the electron storage capacity. The finally electron storage capacity was measured to be 520 μmol electrons per gram of catalyst (assuming that all the stored electrons are fully used for H_2 production). And more importantly, the photocatalytic performances of these materials are strongly affected by the electron storage capacity, certifying the importance of electron storage for the improvement of photocatalytic performance (Fig. 5b). Expanding the electron storage capacity will lead to the enhanced exciton dissociation and finally lead to the dramatically enhanced photocatalytic performance of CCN. The dark and photocatalytic H_2O_2 generation results in Fig. 5 c and d also confirm the electron storage capacity has positive effect on photocatalytic performance. As we see, the highest photocatalytic activity for both H_2 evolution and H_2O_2 production is observed on the material with highest electron storage capacity.

Alerting the introduced amount of alkali metal ions may be another way to expanding the electron storage capacity. By adding appropriate amount of alkali metal salt into the reaction system, we noticed an unprecedented enhancement of CCN for photocatalytic H_2 evolution whereas no improvement was found for the pristine g-C_3N_4. As displyed in Fig. 6a, CCN exhibits an unprecedented photocatalytic H_2 evolution performance at a rate of 508 μmol/h, while g-C_3N_4 remains unchanged (5.1 μmol/h) by using TEOA as sacrificial agent. This value is even comparable to the state-of-the-art carbon nitride materials for H_2 generation using TEOA as sacrificial reagent under visible light (Table S3). Previous study has assigned this enhancement to the production of Cl/·Cl, which act as an electron shuttle mediator to accelerate the hole capture [25]. However, as we may notice that the production of such shuttle needs the valence band with potential positive than 2.4 eV, which is much positive than the valence band position of g-C_3N_4. Furthermore, such enhancement can only find on the modified g-C_3N_4 while the pristine g-C_3N_4 remains unchanged even if the energy band structures are similar [41]. Here, we have shown that endowing CCN with electron storage can effectively enhance the photocatalytic activities, expanding the electron storage capacity will lead to improvement of exciton dissociation. Furthermore, as we discussed that alkali metal ion intercalation can stabilize the trapped electrons, thus adding alkali metal salt into the system may lead to the expanding of electron storage capacity. As evidenced in Fig. 6b, when adding appropriate amount of alkali metal ion into the system, the electron storage capacity is further expanded and reaches over 1000 μmol/g. With an expanded electron storage capacity, the further enhanced photocatalytic performance of CCN for H_2 evolution is then reasonable. The apparent quantum yield (AQY) of CCN for H_2 evolution in the presence of KCl salt reaches 55% at 420 nm, which is much higher than most of the polymeric materials. When using methanol as hole scavenger, the photocatalytic H_2 evolution performance reaches higher than 100 μmol/h (Fig. 6c), which is also among the highest value of carbon nitride materials by using methanol as sacrificial reagent under visible light (Table S4). This well explained the accelerated photocatalytic activity only achieves on CCN while g-C_3N_4 without electron storage ability keeps unchanged in the alkali metal contained solution.

We have also tested the recyclability of the electron charge-discharge of CCN by the dark catalytic H_2O_2 generation. No obvious decay in the electron storage capacity is found after four cycles of photo charge-discharge process, demonstrating the high structural stability of it (Fig. 6d). Besides, the stored electrons on CCN can persist for several tens of hours, again confirming the high structure stability for electron location. So this kind of material with electron storage ability can also act as a safe energy carrier for transportation and release the energy in the specified chemicals when demand, accordingly. Given the currently limitation of high capacity and safety of solar energy storage mechanisms, this material not only shows great promise in the practical application of solar energy storage and transportation, but also can bring the artificial synthetic devices back to work in light scanty period by using the stored electrons.

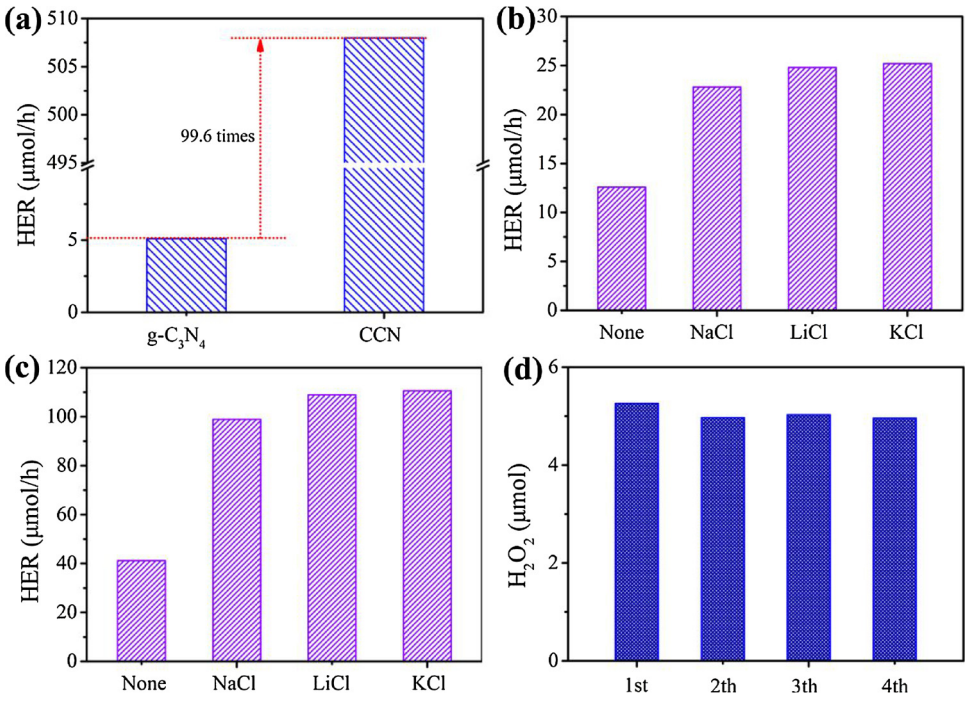

Fig. 6. (a) Photocatalytic H_2 evolution of g-C_3N_4 and CCN using TEOA as sacrificial reagent and in the presence of KCl. (b) Dark H_2 evolution and (c) photocatalytic H_2 evolution of CCN in the presence of different kind of alkali metal salts. (d) Cycle runs of CCN photocatalyst for dark catalytic H_2O_2 generation.

4. Conclusion

In summary, we have shown an electron storage strategy for exciton dissociation to improve the photocatalytic performance of carbon nitride. Endowing carbon nitride with electron storage ability not only can facilitate the exciton dissociation, but also can decouple the redox reactions to inhibit electron-hole recombination. Such a exciton dessociation process can be visualized by the gradually coulour change from yellow to the final blue. We find that expanding the electron storage capacity of CCN would facilitate the exciton dissociation process and therefore dramatically enhance the photocatalytic performance for both H_2 evolution and H_2O_2 generation. This work offers a new way for designing advanced polymeric photocatalytsts toward high performance solar energy conversion via excitonic engineering.

Acknowledgments

This work was supported by National Natural Science Foundation of China (NO. 21590813), the Program of Introducing Talents of Discipline to Universities (B13012), the Program for Chang Jiang Scholars and Innovative Research Team in University (IRT_13R05) and the Fundamental Research Funds for the Central Universities (DUT16TD02).

Appendix A. Supplementary data

Supplementary material related to this article can be found, in the online version, at doi:https://doi.org/10.1016/j.apcatb.2018.05.003.

References

[1] W.J. Ong, L.L. Tan, Y.H. Ng, S.T. Yong, S.P. Chai, Graphitic carbon nitride (g-C_3N_4)-based photocatalysts for artificial photosynthesis and environmental remediation: are we a step closer to achieving sustainability, Chem. Rev. 116 (2016) 7159–7329.
[2] J.L. White, M.F. Baruch, J.E. Pander Iii, Y. Hu, I.C. Fortmeyer, J.E. Park, T. Zhang, K. Liao, J. Gu, Y. Yan, T.W. Shaw, E. Abelev, A.B. Bocarsly, Light-driven heterogeneous reduction of carbon dioxide: photocatalysts and photoelectrodes, Chem. Rev. 115 (2015) 12888–12935.
[3] W. Cui, J. Li, F. Dong, Y. Sun, G. Jiang, W. Cen, S.C. Lee, Z. Wu, Highly efficient performance and conversion pathway of photocatalytic NO oxidation on SrO-clusters@amorphous carbon nitride, Environ. Sci. Technol. 51 (2017) 10682–10690.
[4] V.W. Lau, I. Moudrakovski, T. Botari, S. Weinberger, M.B. Mesch, V. Duppel, J. Senker, V. Blum, B.V. Lotsch, Rational design of carbon nitride photocatalysts by identification of cyanamide defects as catalytically relevant sites, Nat. Commun. 7 (2016) 12165.
[5] X. Wang, K. Maeda, A. Thomas, K. Takanabe, G. Xin, J.M. Carlsson, K. Domen, M. Antonietti, A metal-free polymeric photocatalyst for hydrogen production from water under visible light, Nat. Mater. 8 (2009) 76–80.
[6] Y. Zheng, L. Lin, B. Wang, X. Wang, Graphitic carbon nitride polymers toward sustainable photoredox catalysis, Angew. Chem. Int. Ed. 54 (2015) 12868–12884.
[7] F.K. Kessler, Y. Zheng, D. Schwarz, C. Merschjann, W. Schnick, X. Wang, M.J. Bojdys, Functional carbon nitride materials-design strategies for electrochemical devices, Nat. Rev. Mater. 2 (2017) 17030.
[8] Z. Tong, D. Yang, Z. Li, Y. Nan, F. Ding, Y. Shen, Z. Jiang, Thylakoid-inspired multishell g-C_3N_4 nanocapsules with enhanced visible-light harvesting and electron transfer properties for high-efficiency photocatalysis, ACS Nano 11 (2017) 1103–1112.
[9] H. Yu, R. Shi, Y. Zhao, T. Bian, Y. Zhao, C. Zhou, G.I.N. Waterhouse, L.Z. Wu, C.H. Tung, T. Zhang, Alkali-assisted synthesis of nitrogen deficient graphitic carbon nitride with tunable band structures for efficient visible-light-driven hydrogen evolution, Adv. Mater. 29 (2017) 18.
[10] X. Dong, J. Li, Q. Xing, Y. Zhou, H. Huang, F. Dong, The activation of reactants and intermediates promotes the selective photocatalytic NO conversion on electron-localized Sr-intercalated g-C_3N_4, Appl. Catal. B Environ. 232 (2018) 69–76.
[11] H. Wang, X. Sun, D. Li, X. Zhang, S. Chen, W. Shao, Y. Tian, Y. Xie, Boosting hot-electron generation: exciton dissociation at the order-disorder interfaces in polymeric photocatalysts, J. Am. Chem. Soc. 139 (2017) 2468–2473.
[12] X. Chen, S. Shen, L. Guo, S. Mao, Semiconductor-based photocatalytic hydrogen generation, Chem. Rev. 110 (2010) 6503–6570.
[13] C. Chen, W. Ma, J. Zhao, Semiconductor-mediated photogeneration of pollutants under visiable-light irradiation, Chem. Soc. Rev. 39 (2010) 4206–4219.
[14] A.J. Heeger, Semiconducting polymers: the third generation, Chem. Soc. Rev. 39 (2010) 2354–2371.
[15] S. Brazovskii, N. Kirova, Physical theory of excitons in conducting polymers, Chem. Soc. Rev. 39 (2010) 2453–2465.
[16] H. Wang, S. Jiang, S. Chen, X. Zhang, W. Shao, X. Sun, Z. Zhao, Q. Zhang, Y. Luo, Y. Xie, Insights into the excitonic processes in polymeric photocatalysts, Chem. Sci. 8 (2017) 4087–4092.
[17] J. Barber, A mechanism for water splitting and oxygen production in photosynthesis, Nat. Plants 3 (2017) 17041.
[18] A. Magnuson, M. Anderlund, O. Johansson, P. Lindblad, R. Lomoth, T. Polivka, S. Ott, K. Stensjö, S. Styring, V. Sundström, Biomimetic and microbial approaches to solar fuel generation, Acc. Chem. Res. 42 (2009) 1899–1909.
[19] K.N. Ferreira, T.M. Iverson, K. Maghlaoui, J. Barber, S. Iwata, Architecture of the photosynthetic oxygenevolving center, Science 303 (2004) 1831–1838.
[20] P. Libby, P.M. Ridker, G.K. Hansson, Progress and challenges in translating the biology of atherosclerosis, Nature 473 (2011) 317–325.
[21] V.Wh. Lau, D. Klose, H. Kasap, F. Podjaski, M.C. Pignié, E. Reisner, G. Jeschke,

B.V. Lotsch, Dark photocatalysis: storage of solar energy in carbon nitride for time-delayed hydrogen generation, Angew. Chem. Int. Ed. 56 (2017) 510–514.
[22] G. Liu, T. Wang, H. Zhang, X. Meng, D. Hao, K. Chang, P. Li, T. Kako, J. Ye, Nature-inspired environmental "phosphorylation" boosts photocatalytic H_2 production over carbon nitride nanosheets under visible-light irradiation, Angew. Chem. Int. Ed. 54 (2015) 13561–13565.
[23] H. Kasap, C.A. Caputo, B.C.M. Martindale, R. Godin, V.Wh. Lau, B.V. Lotsch, J.R. Durrant, E. Reisner, Solar-driven reduction of aqueous protons coupled to selective alcohol oxidation with a carbon nitride-molecular Ni catalyst system, J. Am. Chem. Soc. 138 (2016) 9183–9192.
[24] L. Lin, H. Ou, Y. Zhang, X. Wang, Tri-s-triazine-based crystalline graphitic carbon nitrides for highly efficient hydrogen evolution photocatalysis, ACS Catal. 6 (2016) 3921–3931.
[25] G. Zhang, G. Li, Z. Lan, L. Lin, A. Savateev, T. Heil, S. Zafeiratos, X. Wang, M. Antonietti, Optimizing optical absorption, exciton dissociation, and charge transfer of a polymeric carbon nitride with ultrahigh solar hydrogen production activity, Angew. Chem. Int. Ed. 56 (2017) 13445–13449.
[26] X. Li, W. Bi, L. Zhang, S. Tao, W. Chu, Q. Zhang, Y. Luo, C. Wu, Y. Xie, Single-atom Pt as Co-catalyst for enhanced photocatalytic H_2 evolution, Adv. Mater. 28 (2016) 2427–2431.
[27] H. Ou, L. Lin, Y. Zheng, P. Yang, Y. Fang, X. Wang, Tri-s-triazine-based crystalline carbon nitride nanosheets for an improved hydrogen evolution, Adv. Mater. (2017) 29.
[28] H. Gao, S. Yan, J. Wang, Y.A. Huang, P. Wang, Z. Li, Z. Zou, Towards efficient solar hydrogen production by intercalated carbon nitride photocatalyst, Phys. Chem. Chem. Phys. 15 (2013) 18077–18084.
[29] D. Dontsova, S. Pronkin, M. Wehle, Z. Chen, C. Fettkenhauer, G. Clavel, M. Antonietti, Triazoles: a new class of precursors for the synthesis of negatively charged carbon nitride derivatives, Chem. Mater. 27 (2015) 5170–5179.
[30] L. Lin, W. Ren, C. Wang, A.M. Asiri, J. Zhang, X. Wang, Crystalline carbon nitride semiconductors prepared at different temperatures for photocatalytic hydrogen production, Appl. Catal. B Environ. 231 (2018) 234–241.
[31] F. Podjaski, J. Kröger, B.V. Lotsch, Toward an aqueous solar battery: direct electrochemical storage of solar energy in carbon nitrides, Adv. Mater. (2018) 1705477.
[32] A. Vinu, Two-dimensional hexagonally-ordered mesoporous carbon nitrides with tunable pore diameter, surface area and nitrogen content, Adv. Funct. Mater. 18 (2008) 816–827.
[33] G.P. Mane, S.N. Talapaneni, K.S. Lakhi, H. Ilbeygi, U. Ravon, K. Al-Bahily, T. Mori, Dae-Hwan Park, A. Vinu, Highly ordered nitrogen-rich mesoporous carbon nitrides and their superior performance for sensing and photocatalytic hydrogen generation, Angew. Chem. Int. Ed. 56 (2017) 8481–8485.
[34] H. Wang, S. Jiang, S. Chen, D. Li, X. Zhang, W. Shao, X. Sun, J. Xie, Z. Zhao, Q. Zhang, Y. Tian, Y. Xie, Enhanced singlet oxygen generation in oxidized graphitic carbon nitride for organic synthesis, Adv. Mater. 28 (2016) 6940–6945.
[35] M. Yang, Y. Xu, W. Lu, K. Zeng, H. Zhu, Q. Xu, G.W. Ho, Self-surface charge exfoliation and electrostatically coordinated 2D hetero-layered hybrids, Nat. Commun. 8 (2017) 14224.
[36] M.L. Kilpatrick, Formation and decomposation of nitrocyanamide in strong mineral acids, J. Am. Chem. Soc. 69 (1947) 40–46.
[37] V.Wh. Lau, V.Wz. Yu, F. Ehrat, T. Botari, I. Moudrakovski, T. Simon, V. Duppel, E. Medina, J. Stolarczyk, J. Feldmann, V. Blum, B.V. Lotsch, Urea-modified carbon nitrides: enhancing photocatalytic hydrogen evolution by rational defect engineering, Adv. Energy Mater. (2017) 1602251.
[38] G. Liu, G. Zhao, W. Zhou, Y. Liu, H. Pang, H. Zhang, D. Hao, X. Meng, P. Li, T. Kako, J. Ye, In situ bond modulation of graphitic carbon nitride to construct p-n homojunctions for enhanced photocatalytic hydrogen production, Adv. Funct. Mater. 26 (2016) 6822–6829.
[39] D.M. Savory, A.J. McQuillan, Influence of formate adsorption and protons on shallow trap infrared absorption (STIRA) of anatase TiO_2 during photocatalysis, J. Phys. Chem. C 117 (2013) 23645–23656.
[40] H.H. Mohamed, C.B. Mendive, R. Dillert, D.W. Bahnemann, Kinetic and mechanistic investigations of multielectron transfer reactions induced by stored electrons in TiO_2 nanoparticles: a stopped flow study, J. Phys. Chem. A 115 (2011) 2139–2147.
[41] Z. Zeng, H. Yu, X. Quan, S. Chen, S. Zhang, Structuring phase junction between tri-s-triazine and triazine crystalline C_3N_4 for efficient photocatalytic hydrogen evolution, Appl. Catal. B Environ. 227 (2018) 153–160.